Raman Studies of Solution Polyglycine Conformations

Sergei Bykov and Sanford Asher*

Department of Chemistry, University of Pittsburgh, Pittsburgh, Pennsylvania 15260

Received: January 4, 2010; Revised Manuscript Received: March 6, 2010

Polyglycine (polygly) is an important model system for understanding the structural preferences of unfolded polypeptides in solution. We utilized UV resonance and visible Raman spectroscopy to investigate the conformational preferences of polygly peptides of different lengths in water containing LiCl and $LiClO_4$. Lithium salts increase the solubility of polygly. Our study indicates that in solution the conformational ensemble of polygly, as well as central peptide bonds of gly_5 and gly_6, are dominated by the 3_1 extended helix, also known as the polyglycine II conformation (PGII). This preference of the polygly backbone for the PGII conformation in solution is likely a result of favorable interactions between carbonyl dipoles in these extended helices. We found that high concentrations of Li^+ stabilize the PGII conformation in solution, most likely by polarizing the peptide bond carbonyls that makes PGII-stabilizing carbonyl−carbonyl electrostatic interactions more favorable. This ability of Li^+ to stabilize 3_1-helix conformations in solution gives use to the denaturing ability of lithium salts.

Introduction

Polyglycine (polygly) occurs in two major structural forms in the solid state, polyglycine I (PGI) and polyglycine II (PGII). Both are extended conformations with Ramachandran dihedral angles of $\varphi = -150°$, $\psi = 147°$ and $\varphi = -77°$, $\psi = 145°$. These conformations are stabilized in the solid state by intermolecular hydrogen bonding between the amide NH and CO groups.

The PGI structure is similar to that of an antiparallel β-sheet, where the almost fully extended backbone forms hydrogen bonds with two antiparallel neighboring chains approximately in the same plane.[1] In the PGII crystal structure, in contrast, an extended 3_1-helix is hydrogen bonded to the six parallel neighboring chains packed in a hexagonal array.[2] Right-handed 3_1-helix conformations are often called polyproline II conformations (PPII) since this structure was first discovered in polyproline. The PPII extended helix is now believed to dominate the poorly understood denatured solution conformation of proteins.

While the solid state of polygly has been extensively studied, very little is known about polygly solution conformations. Oligoglycines longer than 5 residues are normally insoluble in water. Also gly has no chiral atoms, which means that polygly cannot be studied by CD, the standard method used for secondary structure analysis of peptides and proteins in solution.

In the study here, we utilized LiCl and $LiClO_4$ to increase the solubility of polygly chains in water. Li^+ substantially increases the solubility of gly-based peptides in water. For example, LiBr is often used to dissolve and purify silk peptides/proteins that consist mostly of gly, ala and ser residues.

Experimental data on the conformational preferences of gly-based peptides in solution are very limited. Ohnishi et al.[3] showed that the radius of gyration of a six residue gly-based peptide indicates that it is extended, but its length was estimated to be shorter than that of an ideal β-strand or PGII structure, but longer than that of an ideal α-helix. According to polarized visible Raman and FTIR measurements, gly_3 in D_2O solution forms heterogeneous ensembles of conformations, which include 3_1-helix, α-helix, and β-turns.[4] Takekiyo et al. investigated Ac-Gly-NHMe in water at normal and high pressure and found that the most populated conformation is PPII.[5] Recently, we investigated the conformational preferences of the terminal residues of short oligoglycines in aqueous solution and found that the terminal residues span a broad range of extended conformations with some preference for extended 3_1-helix-like conformations and a significant contribution of β-strand-like conformations.[6]

In the work here, we used UV resonance Raman and visible Raman spectroscopy to investigate the solution conformation of long polygly. We compare the spectra of polygly in solution to known solid state structures.

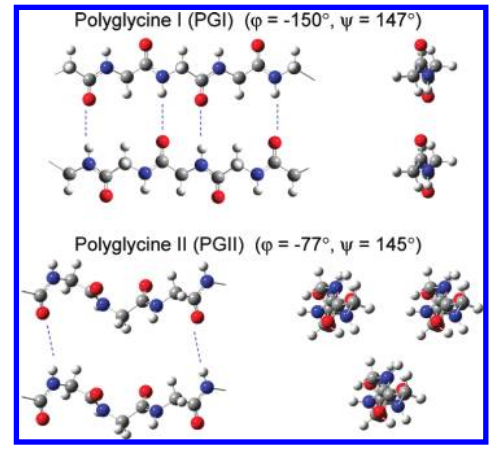

Figure 1. Two conformations of polygly occur in the solid state, β-sheet-like PGI and the extended 3_1-helix PGII.

Experimental Section

Samples. Polygly, MW 500−5000, was purchased from Sigma-Aldrich (St. Louis, MO) and used as received. Lithium chloride (T. J. Baker Inc.) and lithium perchlorate (Fisher Scientific Inc.) were used to increase the solubility of polygly.

* To whom correspondence should be addressed. E-mail: asher@pitt.edu. Tel: 412 624-8570. Fax: 412 624-0588.

10.1021/jp100082n © 2010 American Chemical Society
Published on Web 04/23/2010

Gly_3, gly_5, and gly_6 were purchased from Bachem (King of Prussia, PA) and used as received. Polygly in the PGI and PGII conformations were prepared by precipitation from solution as described elsewhere.[7]

Solution Samples. The 204 nm Raman excitation occurs near the maximum absorbance of the peptide bond $\pi \rightarrow \pi^*$ transition. The third harmonic of a Nd:YAG laser operating at 100 Hz was anti-Stokes Raman shifted in hydrogen to 204 nm (fifth anti-Stokes). The peptides were studied in a flow-stream to avoid contributions from photochemical degradation. Scattered light was dispersed by a double spectrometer and was detected by a Princeton Instruments Spec-10:400B CCD camera (Roper Scientific). A detailed description of the instrumentation is given elsewhere.[8] Excitation of the Raman spectra in the CH stretching region (2700−3200 cm^{-1}) utilized 488 nm Ar-ion laser radiation since CH stretches are not enhanced by deep UV resonance excitation but become overlapped by amide band overtones. A 488 nm holographic notch filter (Kaiser Optical Systems Inc.) was used for Raleigh rejection. We used 10 mg/mL concentrations for the visible Raman measurements. A temperature-controlled fused silica cell (20 mm path length, Starna Cell Inc.) was used for the 488 nm studies.

Solid Samples. For the amide region, we used preresonance 229 nm excitation to minimize sample photodegradation. Raman measurements were performed using an intracavity doubled Ar-ion laser (Coherent Inc.). Scattered light was collected using a backscattering geometry, dispersed by a single monochromator and detected using a Princeton Instruments Spec-10:400B CCD camera (Roper Scientific). Typical accumulation times were less than 1 min. An excitation of 488 nm was used for the CH stretching region. A custom-made, rotating metal cell was used for the solid powder samples to avoid light-induced sample degradation. The powder was pressed into a circular groove in the rotating metal cylinder.

Results

UV resonance Raman spectroscopy is a powerful tool for investigating polypeptide conformation.[9−12] Excitation with deep ultraviolet light within the $\pi \rightarrow \pi^*$ electronic transitions of the peptide bonds results in resonance enhancement of the Raman bands associated with vibrations which distort the peptide bond ground state geometry toward that of the exited state. These amide bands result from polypeptide backbone atom stretching and bending vibrations that makes them sensitive and convenient markers for peptide and protein secondary structure.[10,13]

Gly is a structurally distinct amino acid because it has no C_β atom. This dramatically alters the polygly normal modes compared to the typical amino acid. The UVRR spectrum of gly-based peptides is dominated by five bands in the amide region, the amide I, amide II, amide III, CH_2 wagging, and CH_2 twisting (Figure 2). The amide I band is predominantly peptide bond carbonyl stretching, which is sensitive to the carbonyl environment. The amide II and amide III bands result from complex vibrations of the peptide backbone heavy atoms which are coupled to N−H and $C_\alpha H$ bending. These bands are sensitive to polypeptide conformation and hydrogen bonding to the peptide bond N−H. The CH_2 wagging and CH_2 twisting bands result from $C_\alpha H_2$ deformation vibrations with some contribution from backbone C−C stretching. The CH_2 twisting band is the least sensitive to polypeptide conformation and hydrogen bonding among the amide bands.

Our previous study showed that the terminal residues in oligoglycines span a broad range of extended 3_1-helix-like and β-strandlike conformations.[6] Terminal residues of uncapped

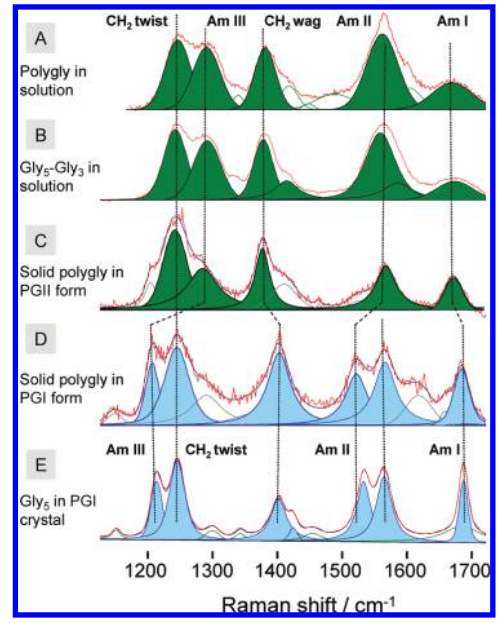

Figure 2. UVRR spectra of polygly. (A) Polygly (~1 mg/mL) in 1.5 M $LiClO_4$ aqueous solution. (B) Gly_5-Gly_3 difference spectrum that approximates the spectra of the middle residues of gly_5 in solution. (C) Solid polygly powder precipitated as mostly PGII. (D) Solid polygly precipitated as mostly PGI conformation. (E) Gly_5 PGI crystalline form. Bands from PGII conformation are marked in green, while PGI conformation bands are in blue.

polypeptides in solution may have distinct conformational preferences due to the electrostatic and steric interactions of the terminal carboxyl and amine groups with the adjacent peptide bonds.

Conformation of Polygly and Internal Residues of Oligogly in Solution. To eliminate the contributions of the terminal residues to the total Raman spectra of polygly, the spectrum of gly_3 was subtracted from those of gly_5 and gly_6. Recently we showed that spectrum of gly_3 closely approximates the spectrum of the two terminal peptide bonds in longer polygly, and that the total UVRR of the oligogly in solution can be treated as a linear sum of the contributing peptide bonds. Thus, the resulting gly_n-gly_3 difference spectra approximate the spectra of the middle residues of the gly_n.

Figure 2 compares the UVRR spectrum of polygly (A) to the gly_5-gly_3 difference spectrum (B). It shows that the UVRR spectrum of high molecular weight (500−5000) polygly, where the contributions from the terminal residues are negligible, is almost identical to the spectrum of gly_5 when the contribution of the terminal residues is subtracted. This result implies that long polygly chains and the central parts of the short oligogly chains populate the same conformational space in aqueous solution. The identical result was obtained for the internal residues of gly_6 (spectra not shown).

To gain insight into the conformational preferences of the long polygly chains in solution we compared the UVRR spectra of polygly in 1.5 M $LiClO_4$ aqueous solution to those of solid polygly samples of known conformation. ($LiClO_4$ is used to increase the solubility of polygly in water and as an internal Raman intensity standard.) Polygly can adopt antiparallel β-sheet-like PGI and extended 3_1-helix PGII in the solid state. These conformations can be obtained by precipitation from solution. Figure 2 shows the UVRRS of polygly in solution and spectra of solid polygly samples in the PG II and PGI conformations.

The CH_2 twisting mode at 1250 cm^{-1} does not show a significant frequency difference between the solid-state PGI and

TABLE 1: UVRR Frequencies and Bandwidths (*w*) of the Amide Bands of Polygly

	polygly in 1.5 M $LiClO_4$ solution		solid polygly, mostly PGII sample		solid polygly, mostly PGI sample		Gly_5, PGI crystal	
	ν/cm^{-1}	w/cm^{-1}	ν/cm^{-1}	w/cm^{-1}	ν/cm^{-1}	w/cm^{-1}	ν/cm^{-1}	w/cm^{-1}
$CH_{2\ twist}$	1254	42	1249	41	1253	43	1249	27
Am III	1300	58	1291	56	1216	24	1219	20
$CH_{2\ wag}$	1386	32	1380	26	1404	41	1400	28
Am II	1562	58	1563	37	1519	39	1525	25
Am I	1667	79[a]	1663	31	1675	28	1674	15

[a] The amide I band of polygly in water is unusually broad, likely due to the residual contribution from the water bending vibration.

PGII conformations, and polygly in solution. In contrast, the amide III band upshifts 75 cm^{-1} from 1216 cm^{-1} for PGI to 1291 cm^{-1} for PGII, in the solid state. The polygly amide III band in solution is at ~1300 cm^{-1}, similar to that of the solid PGII sample. The CH_2 wagging downshifts 29 cm^{-1} (from 1409 to 1380 cm^{-1}) between the PGI and PGII conformations, while the amide II band upshifts 44 cm^{-1}. The amide I downshifts only 8 cm^{-1}. The CH_2 wagging band frequencies and the amide II and amide I band frequencies of polygly in solution (see Table 1) are also very close to those of the solid state PGII conformation. The UVRR data indicate that polygly in aqueous solutions containing Li^+ exist in a conformation close to the PGII extended helix in the solid state. The spectral frequencies of the solid state PGI and PGII conformations agree well with those calculated by Abe and Krimm.[14,15]

Table 1 lists the frequencies for the major conformational-dependent bands of the spectra of polygly in solution as well as for solid PGII and PGI conformations.

Crystalline solid molecular conformations are often determined by crystal packing forces that result in a single well-defined molecular conformation. This explains the much smaller bandwidths (FWHM) of the amide II and amide III bands in the UVRRS of crystalline gly_5 of ~20−25 cm^{-1} (Table 1), as opposed to the polygly in solution FWHM of ~58 cm^{-1}, ~3-fold broader.

Conformation of Polygly and Oligogly in Solution. Evidence from the CH Stretching Region. Since the peptide bond includes highly polar groups such as C═O and N−H, the amide band frequencies depend not only on backbone conformation but also on its hydrogen bonding, which will differ between solid state and solution polygly. The C−H bond is much less polar, which will minimize the dependence of the C−H stretching frequencies on the environment.

We previously showed that the gly $C_\alpha H_2$ group stretching vibrations show a large conformational dependence.[16] In peptides, the conformational sensitivity of the CH_2 stretching frequencies arises from hyperconjugation of the C−H bond molecular orbitals with those of the adjacent peptide bond.

Figure 3 compares the Raman spectra of the CH_2 stretches of polygly in solution and solid state. Table 2 shows the frequencies and bandwidths of the CH_2 stretching bands. The CH stretching region of solution polygly and solid state PGII are very similar. Both show the CH_2 stretch doublet with an intense symmetric stretch at 2936 cm^{-1}, and a less intense asymmetric stretch at 2976 cm^{-1}. The CH_2 stretching doublet of β-sheet-like PGI is red-shifted compared to that of PGII, with the CH_2 symmetric stretch at 2924 cm^{-1} and the asymmetric stretch at 2948 cm^{-1}, showing comparable intensities.

Gly_5 in the PGI conformation shows its symmetric stretch at 2929 cm^{-1} and its asymmetric stretch at 2950 cm^{-1}, similar to polygly, but with narrower bands. The low-intensity bands in the spectrum of gly_5 (marked with the *) are due to the terminal methylene groups where the CH_2 stretching frequencies are shifted by the adjacent amine and carboxyl groups.[16]

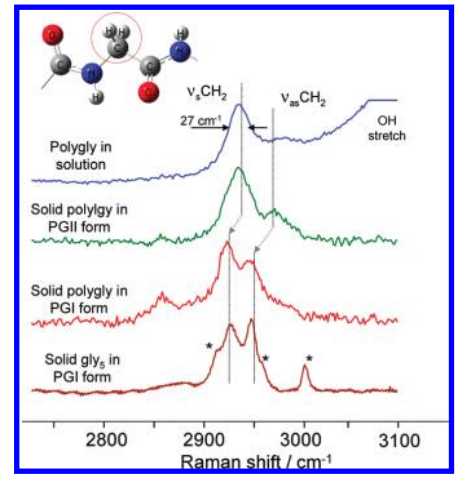

Figure 3. Raman spectra (488 nm) of polygly in 9 M LiCl solution, solid polygly in the PGII form, solid polygly in the PGI form, gly_5 in the PGI form. The spectra of polygly in solution and solid polygly in the PGII form are essentially identical. The homogeneous FWHM of the CH_2 stretch is ~12 cm^{-1} as determined from spectra of gly_5 crystals. The bandwidth of the $\nu_s CH_2$ of the solution sample is more then twice that of crystalline gly, indicating solution conformational inhomogeneity. The structure on the top shows the CH_2 group in a peptide segment in the polygly chain.

As in the case of the amide III band, the bandwidths of the CH_2 stretches of PGII in solution and solid state are significantly broader then those in the PGI form, indicating an increased PGII conformational inhomogeneity.

Discussion

Polygly is the most flexible polypeptide because its lack of side chains removes steric hindrances. The polygly Ramachandran plot shows more allowed regions than for any other amino acid. Because gly is achiral, the sterically allowed regions are symmetric about ($\varphi = 0°$, $\psi = 0°$) which means that conformations with (φ, ψ) and ($-\varphi$, $-\psi$) are identical. Gly can assume virtually any ψ angle while its φ-angle has a forbidden region ($\varphi \sim 0 \pm 60°$) due to adjacent peptide bond carbonyl oxygen clashes.[17]

This high flexibility of polygly chains makes any strictly defined conformations highly entropically unfavorable. Molecular dynamic simulations of gly derivatives, such as Ace-Gly-NMe, show a distribution of conformations with a broad population maxima which depend on the force field used for calculations.[18] In proteins, gly often assumes conformations that are not sterically allowed for other amino acid residues such as a left-handed 3_{10}-helix.[17]

Our Raman data show that both internal residues of short oligoglys and long polygly homopolymers in solution populate Ramachandran angles centered on the PGII ($\varphi \sim -77°$, $\psi \sim 145°$) or 3_1 extended helix, which are not significantly populated for gly in folded proteins.[19,20]

TABLE 2: Gly_n Frequencies and Full Width at Half-Maximum (w) of the $C_\alpha H_2$ Symmetric ($\nu_s CH_2$) and Asymmetric ($\nu_{as} CH_2$) Stretching Bands in Solution and Solid State

	polygly in 9 M LiCl solution		solid polygly, mostly PGII		solid polygly, mostly PGI		gly_5, PGI crystal	
	ν/cm^{-1}	w/cm^{-1}	ν/cm^{-1}	w/cm^{-1}	ν/cm^{-1}	w/cm^{-1}	ν/cm^{-1}	w/cm^{-1}
$\nu_s CH_2$	2937	27	2936	32	2924	19	2929	21
$\nu_{as} CH_2$	2976	35	2976	30	2948	25	2950	13

Effect of Li^+ on Polygly in Solution. Polygly chains longer than five residues are insoluble in pure water. Lithium salts can significantly increase the solubility of polygly. The small Li^+ ions produce strong electrostatic fields and strongly interact with water oxygen atoms to form stable $Li^+(H_2O)_n$ complexes, where n depends on the Li^+ concentration. Some studies indicate that the Li^+ ion can directly bind to the amide groups at the carbonyl oxygens due to the carbonyl group large dipole moment.[21−24] Li^+ may also compete with the peptide bond N−H for hydrogen bonding to water oxygens.

To gain insight into the specific influence of the lithium salts on the peptide bond we investigated the Li^+ induced perturbations in the UVRR spectra of gly_3. Figure 4 shows the spectra of the gly_3 at low (0.3 M) and high (9 M) Li^+ concentrations at 10 and 60 °C. The polypeptide amide band frequencies in aqueous solution are temperature dependent because the increased temperature decreases the peptide bond hydrogen bonding to water.[10,25]

At low (0.3 M) Li^+ concentrations, the gly_3 spectra show the temperature-induced frequency shifts that are typical for a water-exposed peptide bond. In H_2O the amide II and amide III bands are the most temperature dependent and downshift −4.3 and −3.7 cm^{-1} as the temperature increases from 10 to 60 °C. The amide I band slightly upshifts 1.6 cm^{-1} (Figure 4, Table 3). The amide II and amide III band frequencies are sensitive to hydrogen bonding changes since these vibrations have a significant contribution from N−H bending. Temperature increases weaken hydrogen bonding between N−H and water, making the N−H bonds shorter which downshifts the amide II and amide III frequencies.[10] In contrast, weakening of the hydrogen bonding between the peptide bond carbonyl and water results in C═O bond shortening and upshifting the amide I band (C═O stretch). The temperature induced changes in the C═O, C−N, and N−H bond length are schematically shown in Figure 4.

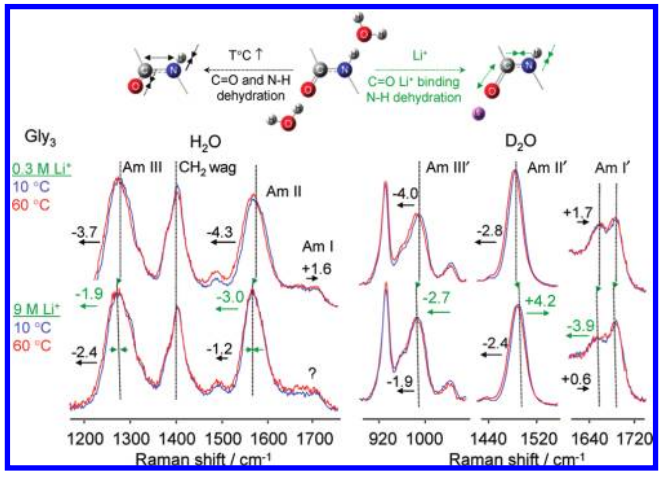

Figure 4. UVRR spectra of gly_3 in H_2O (left) and D_2O (right) at 0.3 M (top) and 9 M (bottom) of Li^+. Blue 10 °C, red 60 °C. H_2O and D_2O contributions are numerically subtracted. The temperature-induced frequency shifts between 10 and 60 °C are shown by black arrows. Green arrows indicate Li^+-induced band shifts and band narrowing at 10 °C. The spectra are arbitrarily scaled. The molecular structures above schematically show the effects of dehydration and Li^+ binding on the carbonyl oxygens on the peptide bond lengths.

At high concentrations of Li^+, the temperature-induced downshifts of the amide II and amide III bands decrease. The amide II band downshifts only by −1.2 cm^{-1} while the amide III band downshifts −2.4 cm^{-1} as the temperature increases from 10 to 60 °C in 9 M LiCl (Figure 4 and Table 3). This decreased temperature dependence of the amide II and amide III bands in concentrated Li^+ solutions indicates a change in the hydrogen bonding to the peptide N−H group.

The amide II band is the most affected by Li^+. At 10 °C the amide II band downshifts −3 cm^{-1} upon increasing the LiCl concentration from 0.3 to 9 M. This downshift is likely due to weakening of the hydrogen bonding between the peptide bond N−H and water, probably due to N−H dehydration. The small Li^+ has a high charge density and complexes with 4−6 water molecules in its first solvation shell. In 9 M LiCl, most of the water molecules oxygens are bound to Li^+ decreasing the hydrogen bonding of water to the peptide bond N−H.

High Li^+ concentrations significantly narrow the amide II bandwidth ∼20% (10.6 cm^{-1}), which indicates a decrease in the gly_3 conformational distribution. The amide III band also narrows ∼5%. This smaller bandwidth change may be due to a smaller amide III sensitivity to conformational alterations. For instance, if a decrease in the conformational distribution results from a stabilization of the 3_1-helix over the β-strand, this would mainly alter the Ramachandran φ angle; the amide III band shows only a small φ dependence.[10]

For additional insight into the Li^+ effect on the peptide bond, we investigated the influence of temperature and lithium salts on the UVRR spectra of the gly_3 in D_2O. In D_2O the O−D bending band is significantly downshifted from the amide I region making it easy to determine the amide I′ frequencies. N−H deuteration also dramatically changes the normal mode compositions of the amide II′ band, which becomes almost a pure C−N stretch.

The amide II′ band response to Li^+ is opposite to that of the protonated amide II band. The amide II′ band upshifts 4.2 cm^{-1} as the concentration of Li^+ increases from 0.3 to 9 M in contrast to the −3 cm^{-1} downshift of the protonated amide II. This opposite frequency response results from the difference in normal mode composition of the amide II and amide II′ bands. Upon peptide bond deuteration the amide II′ completely loses its N−H(D) bending component, and becomes almost a pure C−N stretch. Thus, the hydrogen bonding to the N−D will not directly affect the amide II′ frequency. However hydrogen bonding to the peptide bond N−D and C═O still indirectly affects the C−N bond length and the amide II′ frequencies. For example, strong interaction of Li^+ with the C═O elongates it, which shortens the adjacent C−N bond to increase the amide II′ frequency. The C═O elongation results in a −3.9 cm^{-1} amide I′ band frequency downshift upon the Li^+ concentration increase (Figure 4, Table 4). Note that the amide I band of gly_3 appears as a doublet because the N-terminus and C-terminus amide I frequencies differ.

TABLE 3: Band Frequencies (ν), FWHM (w) Bandwidths, Temperature Dependencies of Band Frequencies ($\Delta\nu/\Delta T$) and Temperature Dependencies of Bandwidths ($\Delta w/\Delta T$) for the Amide Bands in the Raman Spectra of gly_3 in H_2O

	Gly_3 in H_2O, 0.3 M Li^+						Gly_3 in H_2O, 9 M Li^+						effect of Li^+ at 10 °C	
	10 °C		60 °C		$\Delta\nu/\Delta T$	$\Delta w/\Delta T$	10 °C		60 °C		$\Delta\nu/\Delta T$	$\Delta w/\Delta T$	$\Delta\nu$	Δw
	ν/cm^{-1}	w/cm^{-1}	ν/cm^{-1}	w/cm^{-1}	cm^{-1}/°C	cm^{-1}/°C	ν/cm^{-1}	w/cm^{-1}	ν/cm^{-1}	w/cm^{-1}	cm^{-1}/°C	cm^{-1}/°C	cm^{-1}	cm^{-1}
Am III	1276.3	63.8	1272.6	65.3	−0.08	0.03	1274.4	60.4	1272.0	61.5	−0.05	0.02	−1.9	−3.4
Am II	1571.7	62.9	1567.4	63.0	−0.09	0.002	1568.7	52.3	1567.5	55.2	−0.03	0.06	−3.0	−10.6
Am I	1663.5	100.1	1665.1	100.6	0.03									
	1708.9	23.4	1708.5	24.4										

TABLE 4: Band Frequencies (ν), FWHM (w) Bandwidths, Temperature Dependencies of Band Frequencies ($\Delta\nu/\Delta T$) and Temperature Dependencies of Bandwidths ($\Delta w/\Delta T$) for the Amide Bands in the Raman Spectra of gly_3 in D_2O

	Gly_3 in D_2O, 0.3 M Li^+						Gly_3 in D_2O, 9 M Li^+						effect of Li^+ at 10 °C	
	10 °C		60 °C		$\Delta\nu/\Delta T$	$\Delta w/\Delta T$	10 °C		60 °C		$\Delta\nu/\Delta T$	$\Delta w/\Delta T$	$\Delta\nu$	Δw
	ν/cm^{-1}	w/cm^{-1}	ν/cm^{-1}	w/cm^{-1}	cm^{-1}/°C	cm^{-1}/°C	ν/cm^{-1}	w/cm^{-1}	ν/cm^{-1}	w/cm^{-1}	cm^{-1}/°C	cm^{-1}/°C	cm^{-1}	cm^{-1}
Am III′	989.2	33.9	985.2	37.3	−0.08	0.07	986.5	34.1	984.6	34.7	−0.04	0.01	−2.7	0.2
Am II′	1485.4	28.8	1482.6	29.5	−0.06	0.02	1489.6	29.2	1487.2	29.7	−0.05	0.01	4.2	0.4
Am I′	1661.0	49.7	1662.7	52.5	0.03	0.06	1657.1	56.8	1657.7	59.1	0.01	0.05	−3.9	7.1
	1690.5	20.3	1689.8	21.4	−0.01	0.02	1689.9	24.1	1688.7	23.2	0.03	−0.02	−0.6	3.8

The amide II′ and amide III′ bands frequencies lose their conformational sensitivity upon peptide bond N−H deuteration since the N−D and $C_\alpha H$ bending motions do not couple. As a result, the amide II′ amide III′ bands do not show any significant bandwidth change in D_2O upon the Li^+ concentration increase.

Peptide Bond Carbonyl Dipole−Dipole Interaction. Initially, Ramachandran explained the allowed regions of the peptide bond φ and ψ angles in terms of hard sphere repulsions between atoms. But this simple explanation results in significant discrepancies between the expected allowed regions in the classical Ramachandran plot and the observed φ, ψ distributions found in high-resolution protein structures. For example, the steric interactions do not account for the diagonal shape of the α_R and α_L region and for the partitioning of the β-region into two diagonal population maxima, the β-strand and PPII regions. It has been shown that these phenomena can be explained by electrostatic interactions within the polypeptide backbone, particularly dipole−dipole interactions.[26]

Maccallum et al. pointed out the importance of the C═O dipole−dipole interactions in stabilizing β-sheet and PPII conformations.[27] Interactions between N−H dipoles appear to be less important because of the significantly lower N and H atom partial charges. Carbonyl−carbonyl dipole interactions were also shown to stabilize partially allowed conformations of asparagine and aspartic acid residues.[28] Calculations show that for an antiparallel bis-propanone dimer carbonyl−carbonyl interactions energies can be as high as ∼−22 kJ/mol, which is comparable to a medium strength hydrogen bond.[29]

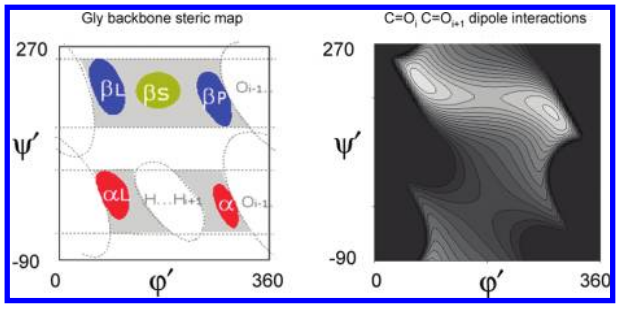

Figure 5. Comparison of the Ramachandran plot and calculated energy map [kcal/mol] of the carbonyl−carbonyl dipole interactions for polygly (light areas correspond to the energy minima). β_L and β_P regions on the Ramachandran plot correspond to 3_1-helix (left and right-handed) energy map minima. This figure was kindly provided by Dr. Bosco Ho.

Ho and Brasseur[30] analyzed the Ramachandran plot of polygly in detail and also calculated electrostatic interactions. They showed that the energy minima in the carbonyl dipole−dipole interaction map correspond to regions populated by 3_1-helix conformations (left and right-handed) in the Ramachandran map (Figure 5).

Thus, the narrowing of the gly_3 conformational distribution observed at high Li^+ concentrations, as indicated by the narrowing of the UVRR amide bands, most likely results from stabilization of 3_1-helix-like conformations in solution. The strong electrostatic fields from the Li^+ cations polarize the peptide bond carbonyls, strengthening peptide bond carbonyl dipole−dipole interactions and making the solution PGII conformation more favorable.

Conclusions

We utilized UV resonance Raman and visible Raman spectroscopy to investigate the conformation of the most flexible polypeptide, polygly in aqueous solution. Our data indicate that long polygly chains (MW 500−5000), as well as the central residues of the gly_5 and gly_6 in solution assume an extended helix PGII-like (or 3_1-helix) conformation. Although polygly chains in solution show a preference for PGII conformations, they still maintain significant conformational freedom, which is apparent from the increased solution bandwidths of the conformationally sensitive amide and CH_2 stretching bands.

High Li^+ concentrations significantly narrow the peptide bond Raman bandwidths, especially that of the amide II band, which indicates a polygly conformational ensemble narrowing which probably results from the stabilization of the PGII conformation by the Li^+ polarization of the peptide bond carbonyls and the strengthening of polypeptide backbone carbonyl dipole−dipole interactions. This Li^+ stabilization of the 3_1-helix-like conformations in solution is likely one of the origins of the protein denaturing ability of lithium salts.

Acknowledgment. We thank Dr. Bosco Ho for permission to use a figure from his publication. This work was supported by the NIH, Grants 5R01EB002053 and 1R01EB009089.

References and Notes

(1) Lotz, B. *J. Mol. Biol.* **1974**, *87*, 169–180.
(2) Crick, F. H. C.; Rich, A. *Nature (London)* **1955**, *176*, 780–781.
(3) Ohnishi, S.; Kamikubo, H.; Onitsuka, M.; Kataoka, M.; Shortle, D. *J. Am. Chem. Soc.* **2006**, *128*, 16338–16344.
(4) Schweitzer-Stenner, R.; Eker, F.; Huang, Q.; Griebenow, K. *J. Am. Chem. Soc.* **2001**, *123*, 9628–9633.
(5) Takekiyo, T.; Imai, T.; Kato, M.; Taniguchi, Y. *Biochim. Biophys. Acta* **2006**, *1764*, 355–363.
(6) Bykov, S. V.; Asher, S. A. J. *Phys. Chem. Lett.* **2010**, *1*, 269–271.
(7) Wildman, K. A. H.; Wilson, E. E.; Lee, D.-K.; Ramamoorthy, A. *Solid State Nucl. Magn. Reson.* **2003**, *24*, 94–109.
(8) Bykov, S.; Lednev, I.; Ianoul, A.; Mikhonin, A.; Munro, C.; Asher, S. A. *Appl. Spectrosc.* **2005**, *59*, 1541–1552.
(9) Balakrishnan, G.; Weeks, C. L.; Ibrahim, M.; Soldatova, A. V.; Spiro, T. G. *Curr. Opin. Struct. Biol.* **2008**, *18*, 623–629.
(10) Mikhonin, A. V.; Bykov, S. V.; Myshakina, N. S.; Asher, S. A. *J. Phys. Chem. B* **2006**, *110*, 1928–1943.
(11) El-Mashtoly, S. F.; Gu, Y.; Yoshimura, H.; Yoshioka, S.; Aono, S.; Kitagawa, T. *J. Biol. Chem.* **2008**, *283*, 6942–6949.
(12) Lednev, I. K. *Methods Protein Struct. Stab. Anal.* **2007**, 1–26.
(13) Kitagawa, T.; Hirota, S. *Handbook of vibrational spectroscopy*; John Wiley & Sons: New York, 2002.
(14) Abe, Y.; Krimm, S. *Biopolymers* **1972**, *11*, 1817–1839.
(15) Abe, Y.; Krimm, S. *Biopolymers* **1972**, *11*, 1841–1853.
(16) Bykov, S. V.; Myshakina, N. S.; Asher, S. A. *J. Phys. Chem. B* **2008**, *112*, 5803–5812.
(17) Lovell, S. C.; Davis, I. W.; Arendall, W. B., III; de Bakker, P. I. W.; Word, J. M.; Prisant, M. G.; Richardson, J. S.; Richardson, D. C. *Proteins: Struct., Funct., Genet.* **2003**, *50*, 437–450.
(18) Hu, H.; Elstner, M.; Hermans, J. *Proteins: Struct., Funct., Genet.* **2003**, *50*, 451–463.
(19) Cubellis, M. V.; Caillez, F.; Blundell, T. L.; Lovell, S. C. *Proteins: Struct., Funct., Bioinformat.* **2005**, *58*, 880–892.
(20) Stapley, B. J.; Creamer, T. P. *Protein Sci.* **1999**, *8*, 587–595.
(21) Balasubramanian, D.; Shaikh, R. *Biopolymers* **1973**, *12*, 1639–1650.
(22) Rodgers, M. T.; Armentrout, P. B. *Acc. Chem. Res.* **2004**, *37*, 989–998.
(23) Imai, T.; Kinoshita, M.; Hirata, F. *Bull. Chem. Soc. Jpn.* **2000**, *73*, 1113–1122.
(24) Bello, J.; Haas, D.; Bello, H. R. *Biochemistry* **1966**, *5*, 2539–2548.
(25) Mikhonin, A. V.; Ahmed, Z.; Ianoul, A.; Asher, S. A. *J. Phys. Chem. B* **2004**, *108*, 19020–19028.
(26) Ho, B. K.; Thomas, A.; Brasseur, R. *Protein Sci.* **2003**, *12*, 2508–2522.
(27) Maccallum, P. H.; Poet, R.; Milner-White, E. J. *J. Mol. Biol.* **1995**, *248*, 361–373.
(28) Deane, C. M.; Allen, F. H.; Taylor, R.; Blundell, T. L. *Protein Eng.* **1999**, *12*, 1025–1028.
(29) Allen, F. H.; Baalham, C. A.; Lommerse, J. P. M.; Raithby, P. R. *Acta Crystallogr., Sect. B* **1998**, *B54*, 320–329.
(30) Ho, B. K.; Brasseur, R. *BMC Struct. Biol.* **2005**, *5*, 14.

JP100082N